Production of Charged Pions in $N-P$ Collisions*†

GAURANG B. YODH‡
Institute for Nuclear Studies, University of Chicago, Chicago, Illinois
(Received January 27, 1955)

The differential cross section and energy spectra for the production of $\pi^{\pm}$ mesons by the 400-Mev neutron beam of the Chicago synchrocyclotron on liquid hydrogen has been measured at 90° and 65° in the laboratory, using photographic emulsions as detectors. At 65° (corresponding to 90° in the center-of-mass system), roughly equal numbers of positive and negative pions were observed, while at 90° the ratio of positive to negative pions was found to be 2.01 ± 0.24. The laboratory integrated cross sections $(d\sigma_{Av}/d\Omega)_{Av}$, in cm²/sterad, are: for π^+ at 90° $(2.296\pm0.363)\times10^{-29}$, for $T>14$ Mev; for π^- at 90°, $(1.56\pm0.357)\times10^{-29}$, for $T>14$ Mev; for π^+ at 65°, $(1.22\pm0.30)\times10^{-29}$, for $T>41$ Mev; and for π^- at 65°, $(1.31\pm0.63)\times10^{-29}$. These experimental cross sections are the result of production due to neutrons of all energies above the threshold for pion production in the neutron beam.

A phenomenological analysis is made for the reaction $N+P\rightarrow\pi^{\pm}$ under the hypothesis of charge independence and the energy and angular distributions of the pions at a single neutron energy are deduced from the experimental cross sections. The total cross section for π^+ or π^- production, at neutron energy 409 Mev, is determined to be

$$\sigma(\pi^+)=\sigma(\pi^-)=0.16\pm0.04 \text{ millibarn},$$

and the differential cross section for the same neutron energy is calculated to be

$$(d\sigma/d\omega)^{\pm}=(1.07\pm0.39)\mp(1.38\pm0.78)\cos\theta+(0.57\pm1.14)\cos^2\theta\times10^{-29} \text{ cm}^2/\text{sterad}.$$

I. INTRODUCTION

ONE of the most significant developments that has been made following the construction of high-energy machines is the artificial production of pions. A considerable effort has been devoted to the study of fundamental processes of pion production in nucleon-nucleon collisions, of which the following are amenable to direct measurement:

$$P+P\rightarrow\pi^++D, \quad (1)$$

$$P+P\rightarrow\pi^++P+N, \quad (2)$$

$$P+P\rightarrow\pi^0+P+P, \quad (3)$$

$$N+P\rightarrow\pi^0+D, \quad (4)$$

$$N+P\rightarrow\pi^0+P+N, \quad (5)$$

$$N+P\rightarrow\pi^-+P+P, \quad (6)$$

$$N+P\rightarrow\pi^++N+N. \quad (7)$$

The processes that have not been most studied are (1) and (2), the production of positive pions in proton-proton collisions. The cross section, angular distribution, and energy spectrum were measured at three angles at 345 Mev by Cartwright, Richman, Whitehead, and Wilcox[1] at Berkeley. Since then the excitation function has been studied by Schulz[2] and Passman, Bloch, and Havens,[3] and careful measurements of reaction (1) have been carried out recently by Crawford and Stevenson[4] at 320 and 345 Mev, by Sutton *et al.*[5] at 430 Mev, and by Rosenfeld[6] at 440 Mev. The production of neutral pions in proton-proton collisions has been studied at only two energies: rather crude measurements of the total cross section have been made at 345 Mev by Mather and Martinelli,[7] and at 430 Mev by Marshall *et al.*[8]

With the availability of the high-energy neutron beam of the University of Chicago synchrocyclotron, a number of experiments were undertaken to study the production of pions in neutron-proton collisions. Hildebrand[9] has studied the production of neutral pions with deuteron formation and also the branching ratio between the reactions (4) and (5). Recently, Schluter[10] has measured the production of neutral pions in neutron-proton collisions using a diffusion cloud chamber, and has also obtained an excitation function for reactions (4) and (5).

The object of the experiment reported in this paper was to measure the production of charged pions in neutron-proton collisions. The energy spectrum and the differential cross sections at 90° and 65° in the laboratory system were measured for both negative and positive pions. Measurements of the same process are being made by Wright and Schluter[11] using a hydrogen diffusion cloud chamber.

These experiments are interesting for the study of pion-nucleon interaction. Pion-production process can be subjected to a phenomenological analysis under

* Supported by the joint program of the Office of Naval Research and the U. S. Atomic Energy Commission.
† Presented in partial fulfillment of the requirements for the degree of Doctor of Philosophy.
‡ Now at Stanford University, Stanford, California.
[1] Cartwright, Richman, Whitehead, and Wilcox, Phys. Rev. **91**, 677 (1953).
[2] A. G. Schulz, University of California Radiation Laboratory Report No. 1756 (unpublished).
[3] Passman, Bloch, and Havens, Phys. Rev. **88**, 1247 (1952).
[4] F. S. Crawford and M. L. Stevenson, Phys. Rev. **97**, 1305 (1955).
[5] Fields, Fox, Kane, Stallwood, and Sutton, Phys. Rev. **95**, 638(A) (1954).
[6] A. H. Rosenfeld, Phys. Rev. **96**, 130 (1954).
[7] J. W. Mather and E. A. Martinelli, Phys. Rev. **92**, 780 (1953).
[8] Marshall, Marshall, Nedzel, and Warshaw, Phys. Rev. **88**, 632 (1952).
[9] R. H. Hildebrand, Phys. Rev. **89**, 1090 (1952); and the results on bound-to-unbound ratio (to be published).
[10] R. A. Schluter, Phys. Rev. **96**, 734 (1954).
[11] S. C. Wright and R. A. Schluter, Phys. Rev. **95**, 639(A) (1954).

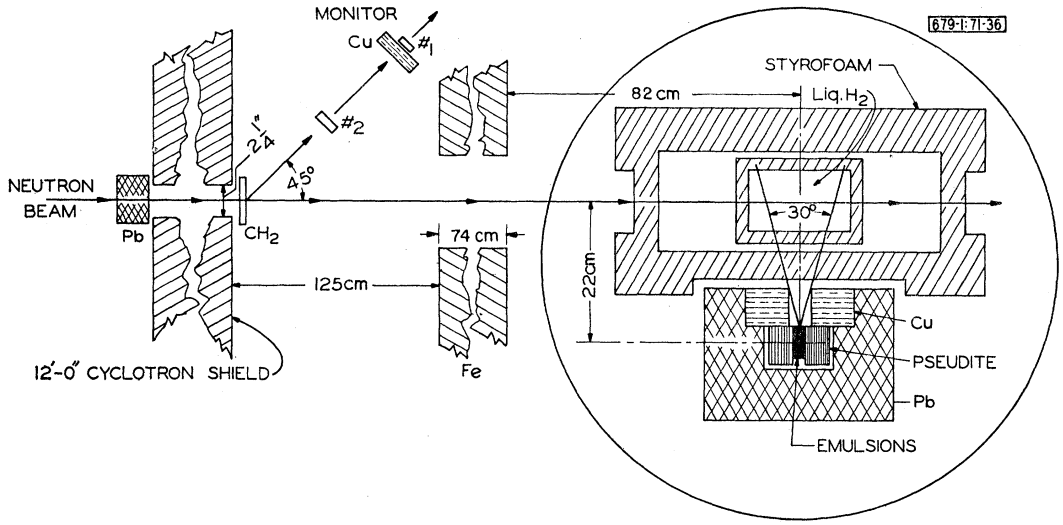

FIG. 1. General arrangement. The emulsion detector geometry for the first run at $\Theta=90\pm15$ is shown in the inset.

charge-independence hypothesis, such as carried out by Brueckner and Watson,[12] and also by Van Hove.[13] They show that it should be possible to describe all these reactions in terms of three fundamental matrix elements. The isotopic spin of the initial state can be zero only in reactions (4) to (7); hence the matrix element for the transition from this state can occur only in these reactions. One of the motivations for the present experiment was to obtain a measure of this matrix element. In addition, it will be of interest to see experimentally how well the charge-independence hypothesis describes the facts.

II. EXPERIMENTAL

This paper is a report of an experiment in which the production of $\pi^{\pm}$ mesons by 400-Mev neutrons interacting with liquid hydrogen was measured using photographic emulsions to detect the mesons.

A. General Arrangement

The 400-Mev neutron beam of the Chicago synchrocyclotron was used in this experiment. This neutron beam is produced by the circulating proton beam of the cyclotron by striking a Be target 2 in. long in the beam direction and 1 in. high. The neutrons selected were those emitted in the forward direction and defined by collimators placed at two ends of the neutron channel through the shielding wall of the cyclotron. The collimation produced a $2\frac{1}{2}$-in. diameter neutron beam at the center of the hydrogen target. Two inches of lead were placed in the path of the beam before the collimation in order to remove electron and gamma-ray contamination of the beam. The general layout is shown in Fig. 1.

The neutron beam was monitored by having it pass through a 1-cm thick polyethylene target, the recoil protons from which were counted by a telescope of two counters (Fig. 1).

Eight feet from the monitor target, neutrons struck a liquid-hydrogen target. An extra 3-ft thick iron shield protected the detectors from neutrons scattered from the end of the collimator or the monitor target. Positive and negative pions produced at 90° and 65° in the laboratory system struck a stack of nuclear emulsions placed at about 22 cm from the center of the hydrogen target. They were brought to rest in the emulsion and the density of track endings was measured as a function of pion range in the emulsion. Negative pions were identified by observing stars at the end of the track, and positive pions from $\pi^{+}\rightarrow\mu^{+}$ decay. The total number of pions leaving the hydrogen at a given angle, and their energy distribution, were obtained from the density of endings.

B. Neutron Beam

1. *Energy Spectrum.*—The neutron beam from a Be target is not monoergic; hence it was necessary to make a measurement of the neutron energy spectrum, which was obtained from a range measurement of the recoil protons from liquid hydrogen.

The neutron beam, collimated to $1\frac{1}{2}$-in. diameter, struck a liquid-hydrogen target.[14] The target used was $3\frac{3}{4}$ in. in diameter with a 5-mil stainless-steel wall, having an outside container with walls of 15-mil duraluminum. The range spectrum of recoil protons from the liquid hydrogen at 20° and 30° was measured by means of a telescope of four counters (see Fig. 2). The solid angle was defined by counter 2 which was placed 50 in. from the center of the hydrogen target,

[12] K. M. Watson and K. A. Brueckner, Phys. Rev. 83, 1 (1951).
[13] Van Hove, Marshak, and Pais, Phys. Rev. 88, 1211 (1952).
[14] The target used here was designed and built by Dr. M. Glicksman and is described in his paper, Phys. Rev. 94, 1335 (1954).

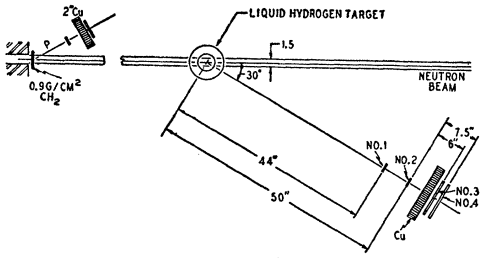

FIG. 2. Experimental arrangement for the measurement of the neutron spectrum.

subtending an angle of 0.04 radian. For this experiment, the neutron beam was monitored by counting recoil protons, emitted at 30° from a 0.9 g/cm² CH_2 target by means of a counter telescope of two counters. Double coincidences of these counters are denoted by M. The beam intensity was also monitored by two auxiliary monitors: (1) a BF_3 counter, which counted slow neutrons in the experimental area, and (2) a thermocouple which measured the heat dissipated in the neutron-producing target.

The quadruple coincidences Q of counters 1, 2, 3, and 4 per monitor count M were recorded for various thicknesses of copper absorbers placed between counters 2 and 3. The absorbers were placed as close to counter 3 as possible to minimize the corrections for multiple and diffraction scattering. The ratio Q/M as a function of x, the thickness of Cu, gives the range curve for the recoil protons. The two range curves for 20.25° and 30° are plotted in Fig. 3. These curves were differentiated to obtain the differential range curves $d\nu/dx$ for the recoil protons.

The energy of the protons at the center of the hydrogen target was calculated from their range in copper by using Aron's tables.[15] The range was obtained from the observed thickness of copper by adding 2.62 g/cm² of copper equivalent due to energy loss in counters 1, 2, 3, and part of 4, in the walls of the target and in half of the liquid hydrogen.

From the curve of $d\nu/dx$, the neutron spectrum is calculated by the equation:

$$\frac{d\nu}{dx}=\frac{dn}{dT_N}\frac{dT_N}{dT_P}\frac{dT_P}{dx}N_H\Delta\Omega_l\left(\frac{d\sigma}{d\Omega}\right)_P\exp\left(-\int_0^x\sigma_{Cu}Ndx\right),$$

where x is the thickness of copper in g/cm²; dn/dT_N is the number of neutrons in the beam, of energy T_N, per monitor count, per Mev; N_H is the number of hydrogen atoms per cm² in the beam; $\Delta\Omega_l$ is the laboratory solid angle; $(d\sigma/d\Omega)_P$ is the differential cross section for producing recoil protons at Θ in the laboratory for neutrons of energy T_N; and $\exp(-\int_0^x\sigma_{Cu}Ndx)$ is the loss of protons due to absorption in thickness x of copper (N is the number of copper atoms per gram). This exponential was calculated using the values of σ_{Cu} (absorption) measured by Kirschbaum.[16] The multiple and diffraction scattering losses of protons were negligible in the geometry used. The laboratory cross section for producing a recoil proton at an angle Θ is given by

$$\left(\frac{d\sigma}{d\Omega}\right)_P=\left[\frac{d\sigma(\phi)}{d\omega}\right]_n\cdot\frac{d\omega}{d\Omega},$$

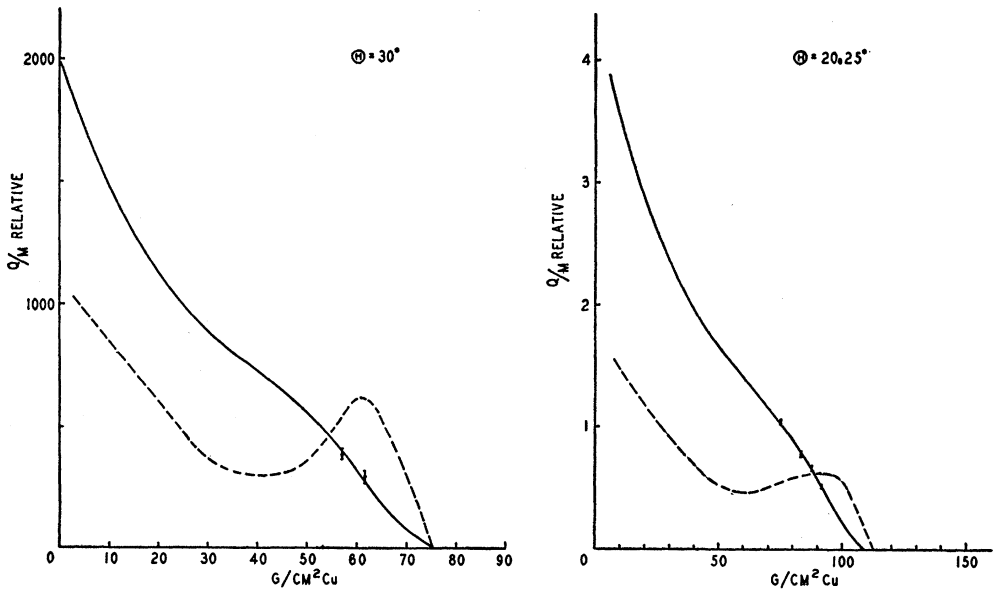

FIG. 3. Integral and differential range curves for recoil protons at $\Theta=20.25°$ and 30°.

[15] W. A. Aron, University of California Radiation Laboratory Report No. 1325 (unpublished).
[16] A. J. Kirschbaum, University of California Radiation Laboratory Report No. 1967 (unpublished).

where $[d\sigma(\phi)/d\omega]_n$ is the differential $N-P$ scattering cross section for giving a recoil proton at Θ in the laboratory or a neutron at the corresponding center-of-mass angle ϕ, and $d\omega/d\Omega$ is the center-of-mass laboratory solid angle transformation. Measured values[17–20] for the cross section $(d\sigma(\phi)/d\omega)_n$ are plotted against the neutron energy T_N in Fig. 4 and a smooth curve drawn through them for obtaining $(d\sigma/d\omega)_n$ at all neutron energies. In calculating the neutron spectrum the errors in the measurement of $(d\sigma/d\omega)_n$ were not included.

The neutron spectra dn/dT_n calculated from the measurements at $\Theta=20.25°$ and 30° are plotted in Fig. 5, and they agree well, within statistical errors. The spectrum shows a sharp high-energy peak with a 10 percent full width at half-maximum. In Fig. 6 is plotted the neutron spectrum $g(t_0)$ normalized to unity for the area from $T_N=280$ Mev to maximum possible neutron energy $T_{N\text{maximum}}=440$ Mev. The abscissa is the maximum meson energy t_0 in the center-of-mass system corresponding to a neutron energy T_N. This energy t_0 is slightly different for π^+- and π^--mesons but for the energy resolution of the experiment the same mean value is assumed for both. This function $g(t_0)$ was analytically approximated by a straight line and a parabola as shown in Fig. 6.

The analytical expressions are given by

$$g_{\mathrm{I}}(t_0)=(0.125t_0+9.65)\times10^{-3},\quad 0<t_0<29\text{ Mev},$$
$$g_{\mathrm{II}}(t_0)=[25.4-0.0772(45-t_0)^2]\times10^{-3},\quad 27<t_0<63\text{ Mev},\qquad(8)$$

where

$$\int_0^{t_0(\text{maximum})} g(t_0)dt_0=1.$$

These functions, when multiplied by the total number of neutrons incident on the hydrogen, give the number of neutrons per unit meson energy in the center-of-mass system.

2. *Neutron Monitor.*—The neutron flux was measured by counting the recoil protons from a 1-cm thick polyethylene target placed in the neutron beam 8 ft ahead of the liquid-hydrogen target (see Fig. 1). The recoil protons were counted by means of a telescope of two counters, with 19.79 g/cm² copper absorber in front of counter 2 which made the telescope sensitive to recoil protons from neutrons of energy greater than 280 Mev only. (This arrangement is shown in Fig. 7.) The counter voltages were set to be in the middle of the plateau curves of double coincidences against counter voltages. The telescope was at 45°±3° to the neutron beam.

[17] Hadley, Kelly, Leith, Segrè, Wiegand, and York, Phys. Rev. **75**, 351 (1949).
[18] Kelly, Leith, Segrè, and Wiegand, Phys. Rev. **79**, 96 (1950); **83**, 923 (1951).
[19] Brueckner, Hartsough, Hayward, and Powell, Phys. Rev. **75**, 555 (1949).
[20] J. de Pangher, Phys. Rev. **92**, 1084 (1953).

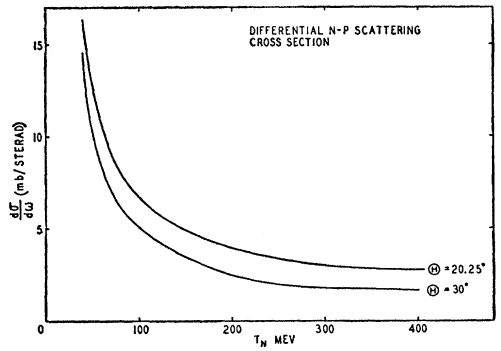

FIG. 4. Differential cross section in the center-of-mass system for scattering a proton at $\Theta=20.25°$ and 30° in $N-P$ collisions.

The number of recoil protons coming from the H_2 in CH_2 were determined by measuring the difference CH_2-C, using a carbon target having the same number of C atoms per cm² as the polyethylene target. The measurement of the ratio $(CH_2-C)/CH_2$ was done at three different times during the experiment and was found not to vary outside statistics. Its value was

$$(CH_2-C)/CH_2=R=0.383\pm0.0146.$$

Thus the number of protons from H_2 are the total number of counts from CH_2 multiplied by R.

To calculate the number of neutrons incident on the H_2, it is necessary to estimate the efficiency of the proton telescope. The counters were nearly 100 percent efficient, and the efficiency of the proton telescope was estimated to be 80 percent, mainly as a result of the loss of protons in the copper and the first counter by absorp-

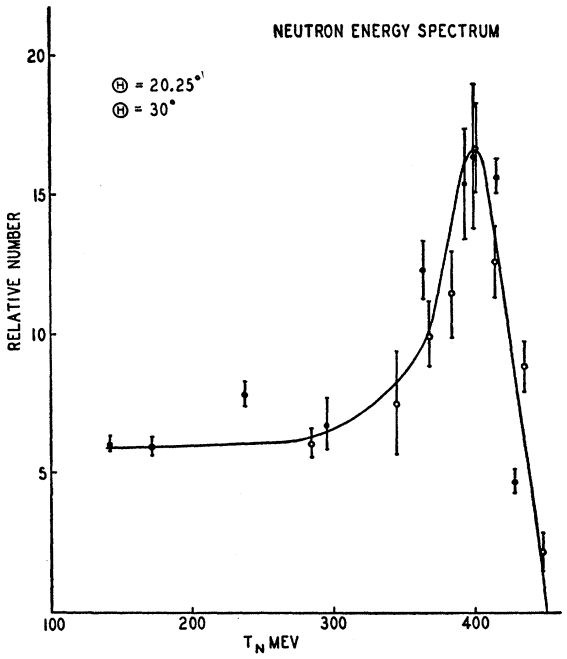

FIG. 5. Energy spectrum of the neutron beam.

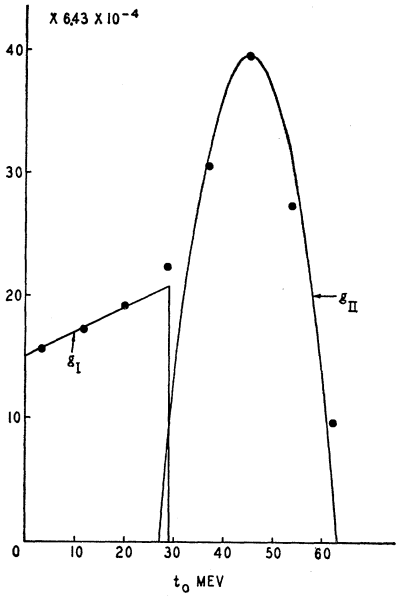

FIG. 6. Neutron energy spectrum as a function of the maximum pion energy in the center-of-mass system.

tion. The number of neutrons incident on the hydrogen are then calculated from

$$N_n=\frac{1}{N_H\Delta\Omega(d\omega/d\Omega)(d\sigma/d\omega)_n}\frac{\nu_p R}{\epsilon},$$

where ν_p is the total number of counts from hydrogen; ϵ is the efficiency of the telescope ($\epsilon=0.80$); N_H is the number of hydrogen atoms per cm^2 in CH_2 target ($N_H=7.924\times10^{22}$); $\Delta\Omega$ is the solid angle subtended by counter 2 ($\Delta\Omega=2.5\times10^{-3}$ sterad); $d\omega/d\Omega$ is the solid angle transformation from the laboratory system to the center-of-mass system ($d\omega/d\Omega=2.81$); and $(d\sigma/d\omega)_n$ is the $N-P$ differential cross section for producing recoil protons at $\Theta=45°$ in the laboratory: $(d\sigma/d\omega)_n=1.58\pm0.047$ mb/sterad.

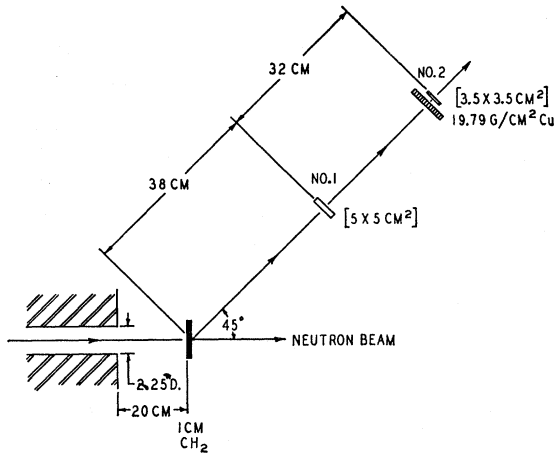

FIG. 7. Monitor geometry.

The differential cross section $(d\sigma/d\omega)_n$ was calculated at 400-Mev neutron energy using the measured value of the total $N-P$ cross section by Nedzel[21] and the angular distribution by Hartzler and Siegel.[22] The Berkeley value[19] was used at 280 Mev. The error in the knowledge of $(d\sigma/d\omega)_n$ is 3 percent. For the two exposures made, the total number of neutrons incident on the target for the effect and the background runs are given in Table I.

C. Hydrogen Target

A double-walled Styrofoam target, based on an original design by Marshall,[23] was used (Fig. 8). The outside container had 3-in. thick walls except where the beam passed through, where it was $1\frac{1}{2}$ in. thick. It was also thinned down to 2 in. where the pions emerged at 65° to the beam. The inside container had 1-in. thick walls, and it was 8 in. long, 4 in. wide and 6 in. deep. Both containers were lined by 2-mil aluminum foil. The linings distributed the cold over the Styrofoam evenly to prevent thermal strains. The cold hydrogen vapor circulates around the inner container and then goes out of the hole at the bottom through an oil trap and gas meter to the exit. The level of the hydrogen was observed by measuring the level of a Styrofoam float C, noting the height of the balsa-wood stick in the Pyrex tube F. Liquid hydrogen is transferred through E. The two ends of the target were aligned with respect to the beam to within 1 mm.

The target had three important features to make it suitable for this experiment: (1) The hydrogen container was made long enough in the direction of the beam so that the walls through which the neutron beam passed were not directly visible by the detector. (2) The thicknesses of the Styrofoam walls in the beam were reduced so as to minimize the production of mesons from the walls. (3) The low density of Styrofoam makes the energy loss of pions passing through them small so that the energy threshold of the detector can be lower than otherwise.

D. Emulsion Detector

The detector consisted of a stack of stripped Ilford G-special emulsions, 1800 microns thick, placed at 22 cm from the center of the target at 90° and 65° to the neutron beam (Fig. 9). The pellicles (emulsions stripped from glass backing) were embedded in a holder of

TABLE I. Total number of neutrons incident on the target.

Target	Run A in units of 10^{11}	Run B in units of 10^{11}
With hydrogen	1.508±0.050	5.706±0.196
Without hydrogen	1.109±0.036	1.199±0.041

[21] V. A. Nedzel, Phys. Rev. **91**, 440 (1953).
[22] A. J. Hartzler and R. T. Siegel, Phys. Rev. **95**, 185 (1954).
[23] L. Marshall (to be published).

material, "pseudite,"[24] which has the same density, stopping power, and radiation length as that of the emulsion. The size of the emulsions at each angle was determined by the requirement that the maximum-energy pion at that angle would come to rest in the emulsion. The pellicles were 1.5 in. long for the 90° stack and 4 in. for the 65° stack.

The G-special emulsions are most suited for this type of experiment because they are insensitive to electrons, and they have higher sensitivity than C-2 emulsions, high enough to make the meson tracks sufficiently heavy and the variation in grain density near the end of the track rapid enough to produce very distinctive pion endings. Further, there is a marked change in grain density between the pion track at its end and the emitted muon track. This makes identification of $\pi^+ \rightarrow \mu^+$ decay immediate. Pellicles 1800 microns thick were used for the following reasons: (1) to be able to identify each π^+ ending by following the muon to its end, which was achieved by scanning only the middle third of the emulsion; (2) to halve the time of development and to permit more uniform development than for plates of equal thickness; (3) to avoid the presence of material different from emulsion in the detector stack.

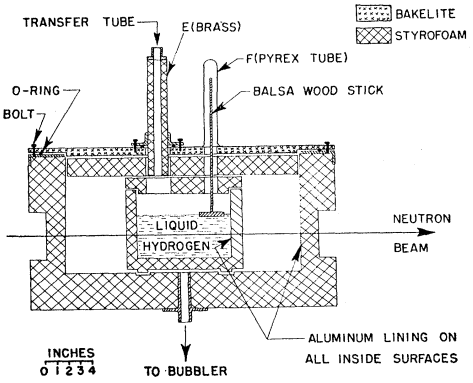

FIG. 8. Styrofoam liquid-hydrogen target.

The angular acceptance at each angle was determined by means of copper or lead collimators (Fig. 9). The angular spread was $\pm 15°$ for $\Theta = 90°$ for the first run and $\pm 5°$ and $\pm 3°$ for $\Theta = 90°$ and 65°, respectively, for the second run. A lead collimator with 1 cm of tungsten in the front edge was used on the upstream side of the 65° stack because the high densities of these materials could make the angular definition sharper by stopping high-energy particles in a small thickness.

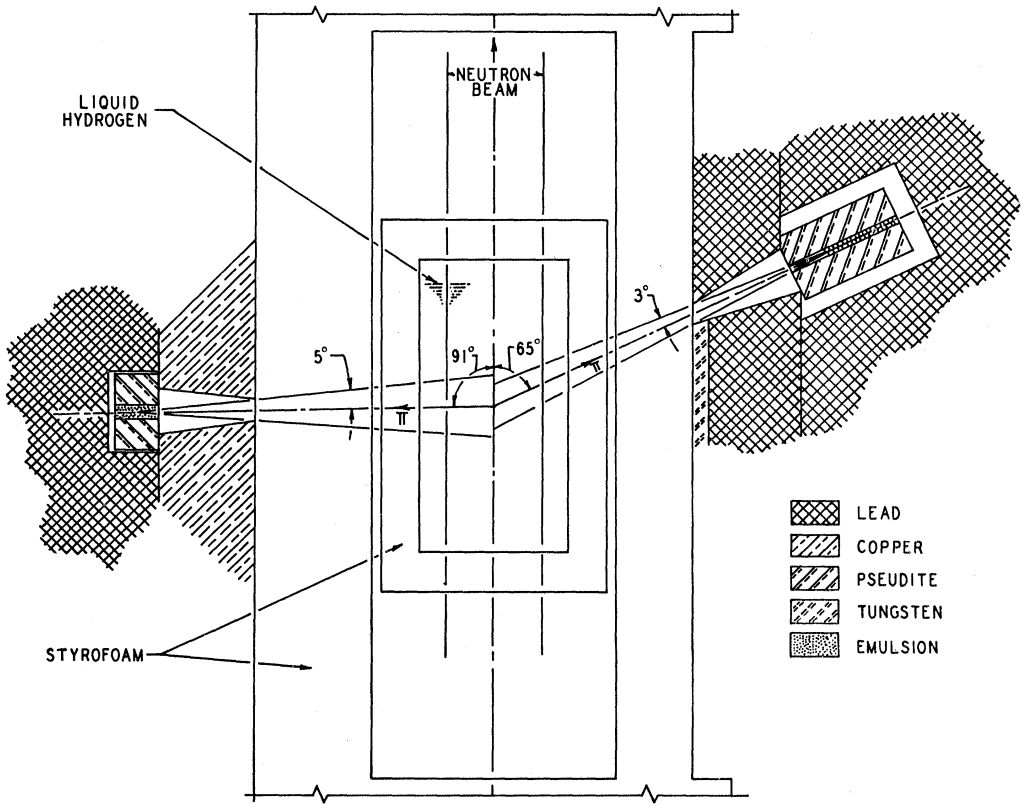

FIG. 9. The 91° and 65° geometries used in the second run.

[24] Pseudite is a machinable, molded mixture of fine Cu, Sn, and Lucite powders, 150 mesh or smaller. Each cc contains 1.28 g Cu, 1.94 g Sn, and 0.71 g Lucite, and has a total density of 3.93±2 percent. See Rosenfeld, reference 6.

E. Exposure and Scanning

1. *Exposure.*—Two exposures were made. The first was made at 90°±15° in order to determine the magnitude of the cross section and to get an idea of the background. The background, measured without hydrogen in target, was very low and permitted improving the angular resolution three-fold. This was done in the second exposure. Exposures were made at two angles: 91°±5° and 65°±3°.

At 91° there are no recoil protons from the hydrogen due to $N-P$ scattering, permitting one to scan all the way to the edge of the emulsion obtaining lowest possible threshold for the pions. For angles larger than 90°, the energy of the pions becomes too low to measure the pion spectrum adequately.

At 65° there is sufficient difference between the ranges of the maximum-energy recoil protons due to $N-P$ scattering and that of the pions to make scanning for pions beyond the proton range possible. The energy threshold of detection determined by the range of the maximum-energy recoil proton was 41 Mev. For smaller angles the number of recoil protons and neutrons becomes very large and their energy becomes high so that the plate would become impossible to scan because of too many extraneous events. Furthermore, the center-of-mass angle corresponding go the laboratory angle 65° is close to 90° so that the constant term a in the angular distribution $(a+b\cos\theta+c\cos^2\theta)$ can be determined directly (see Sec. VI, below).

The length of the second exposure was adjusted so as to obtain the same density of pion endings at 90° as in the first exposure. At both angles exposures were made with and without liquid hydrogen in the target, care being taken to have only hydrogen gas in the target during the background exposure.

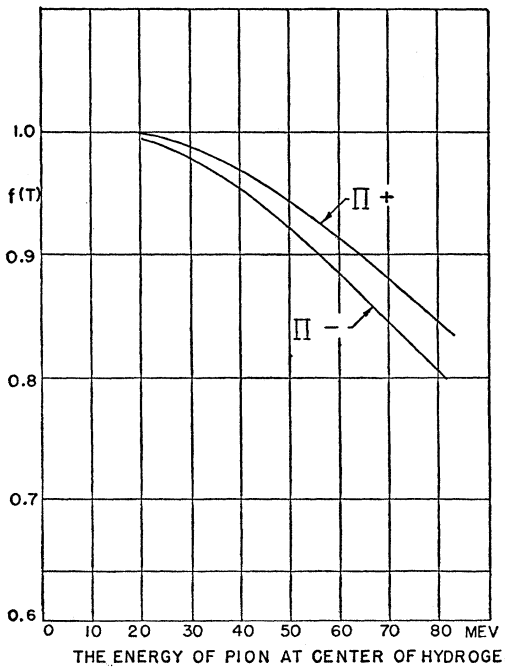

FIG. 10. Nuclear absorption correction as a function of the pion energy in the laboratory at the center of the hydrogen target.

2. *Scanning.*—The method of observation was to scan the emulsion using 22×oil objectives (also 12.5×oil objectives for the background plates) in strips starting from the threshold of detection, along the direction of pion incidence up to about 5 mm beyond the range of the maximum-possible-energy pion. For each strip only the middle 600 microns of the emulsion were scanned. Both pion and muon endings in this layer were recorded. This insured that whenever a $\pi^+\rightarrow\mu^+$ decay was found it was possible to follow the muon to the end of its range, 597±28 microns,[25] and thus identify the event unambiguously. For negative pions all π^- stars with one or more prongs were recorded. The number of no-pronged negative-pion endings were calculated by using the value[26] 1.36 for the ratio of the total number of negative-pion endings to the number of pion endings with stars having one or more prongs.

The advantage of scanning the middle 600 microns of a pellicle 1800-microns thick is that it permits a truly objective test of scanning efficiency.[27] If a $\pi^+\rightarrow\mu^+$ decay is found in this 600-micron layer, there is about 50 percent probability that the associated muon will also end in the same layer, though not necessarily in the strip currently being scanned, because the range of the muon is equal to the thickness of the layer. Therefore, one-half of the pions found by direct scanning in this layer should lead back to muons in the same layer. Similarly, one-half of the muons found in this layer by direct scanning should lead back to pions in the same layer. Thus pions are found in two independent ways: By direct scanning and via muons. If the scanning efficiency were 100 percent it should never happen that a pion is seen only by tracking the corresponding muon and is missed in the direct search. The scanning efficiency for pions found by direct scanning is then given by $1-(N_m/N_t)$, where N_m is the number of pions missed by direct observation but found by tracking. A similar efficiency check was kept for the muons. For example, in the first exposure about 50 pions and muons were tracked. The number missed was 3 pions and 3 muons, giving an efficiency of 94 percent for both pions and muons. For the negative pions no such efficiency test is possible and the scanning efficiency was assumed to be equal to that for the positive pions.

For the 90° experiment the event rate was about 1 event every 10 minutes under 22×oil objective. The 65° exposure, however, had a high background of

[25] W. F. Fry, Phys. Rev. **83**, 1268 (1951).
[26] F. L. Adelman and S. B. Jones, Phys. Rev. **75**, 1468(A) (1949); A. H. Rosenfeld and W. F. Fry (private communication); W. Dudziak, University of California Radiation Laboratory Report UCRL-5641, 1954 (unpublished).
[27] The scanning efficiency test was designed by A. H. Rosenfeld, see reference 6.

proton tracks and stars due to neutrons entering the emulsion, and made scanning much more difficult, reducing the event rate to 1 event every $1\frac{1}{2}$ hours under the same magnification. It was possible to scan the background plates eight times faster than the effect plates. The optimum division of scanning time between effect and background plates required that equal time be spent scanning each of them for best statistics.

A certain fraction of the pions, positive and negative, were not observed in scanning either because they were absorbed by nuclei of the emulsion or suffered large-angle scattering. In the first case they disappear suddenly, and in the latter case they appear coming from the wrong direction. Figure 10 shows curves for the fraction of pions of energy T removed as a result of nuclear absorption and scattering as a function of the energy of the pion at the center of the hydrogen target. They are based on data on nuclear-absorption cross section of pions in emulsion at various energies.[28] Hence, from the observed density of pion track endings as a function of range in emulsion, pion range spectra were determined at two angles. The energy spectra of the pions were obtained by calculating what energy pion, starting at the center of hydorgen, ends at a given range in the emulsion.

F. Energy Resolution

The energy of a pion is determined from its range. This energy is not uniquely determined because of energy spreads due to: (1) straggling, (2) multiple scattering, and (3) variation in energy loss due to size of the beam.

The energy spread due to straggling of the range has a Gaussian distribution. The standard deviation of the straggling distribution has been calculated by using the formula:[29]

$$\frac{[\langle(R-\bar{R})^2\rangle_{\text{Av}}]^{\frac{1}{2}}}{\bar{R}}=\left(\frac{200m_e}{\mu}\right)^{\frac{1}{2}}f\left(\frac{E}{\mu c^2}\right),$$

where μ is the meson mass; the function f is taken from Rossi.[29] The energy spread due to multiple scattering does not have a Gaussian distribution; however, we have approximated the distribution by a Gaussian with 5-percent standard deviation. The spreading of the energy due to the size of the beam occurs because pions produced at different positions in the hydrogen suffer different energy losses in traversing the hydrogen. This energy spread is distributed almost uniformly. The three distributions were folded into each other and the width corresponding to the half-area point of the resultant distribution was calculated. Table II gives the energy spreads for different pion energies at the two angles of the experiment.

TABLE II. Energy resolution. Energy spreads are half-widths the laboratory system.

Laboratory angle	Pion energy in c.m. system (Mev)	Pion energy in lab. system (Mev)	Energy spread in Mev due to: Beam size	Multiple scattering	Straggling	Total spread (Mev)
90°	30	14.5	4.37	0.1	0.08	2.30
	40	23.5	3.00	1.1	0.60	1.55
	50	32.5	2.41	2.0	0.90	1.75
	60	41.5	2.10	2.5	2.00	2.00
65°	30	31.7	2.63	0.40	0.30	1.65
	40	42.0	2.32	1.50	1.00	2.10
	50	57.1	2.01	3.00	2.00	2.65
	60	70.0	1.83	4.80	3.00	3.85

III. CALCULATION OF THE LABORATORY CROSS SECTION

The energy spectra for π^+ and π^- mesons were observed at laboratory angles 90° and 65°. The pion spectra are the result of production due to neutrons of all energies above the threshold of pion production. First, these observations are reduced in terms of experimental cross sections for the particular neutron beam used in this experiment. An effort is then made (see Secs. V, VI, and VII) to reduce these experimental cross sections to center-of-mass cross sections for a single neutron energy.

Each element dv' of the active volume of the target produces

$$\nu_n\rho_{\text{H}}dv'\frac{A}{r^2}\frac{d^2\sigma_{\text{Av}}}{d\Omega dT}$$

pions of energy T into a solid angle A/r^2 at an angle Θ (see Fig. 11). Here $A\cdot\Delta R$= the volume of emulsion scanned for pions of energy T and $T+\Delta T$ which end in the emulsion between range R and $R+\Delta R$. $1/r^2(T,x',y',z')$= distance of the element dv' of the target from the point where a pion of energy T stops in the emulsion. ν_n= number of neutrons/cm^2 incident on the target. ρ_{H}= effective density of liquid hydrogen $=0.0705$ g/cc. $d^2\sigma_{\text{Av}}/d\Omega dT$= cross section for pion production at an angle Θ to the neutron beam, averaged over the neutron spectrum. The density dn/dT of pion tracks of energy T observed in the emulsion will be this number multiplied by: (1) the scanning efficiency ϵ, (2) the probability of decay in flight $\eta(T)$, and (3) the probability of loss due to nuclear absorption in emulsion $f(T)$; and integrated over the active volume of the target:

$$\frac{dn}{dT}=\nu_n\rho_{\text{H}}\epsilon\eta(T)f(T)\int_{\text{target}}dv'\frac{A}{r^2}\cdot\frac{d^2\sigma_{\text{Av}}}{d\Omega dT}. \quad (9)$$

The integral has been approximated by replacing $1/r^2$ and $d^2\sigma_{\text{Av}}/d\Omega dT$ by suitable averages over the target,

[28] G. Bernardini and F. Levy, Phys. Rev. **84**, 610 (1951); Bernardini, Booth, and Lederman, Phys. Rev. **83**, 1075 (1951); Hugh Bradner and Bayard Rankin, Phys. Rev. **87**, 547 (1952); D. H. Stork, Bull. Am. Phys. Soc. **27**, No. 6, 16 (1952).

[29] B. Rossi, *High-Energy Particles* (Prentice-Hall, Inc., New York, 1952), p. 37.

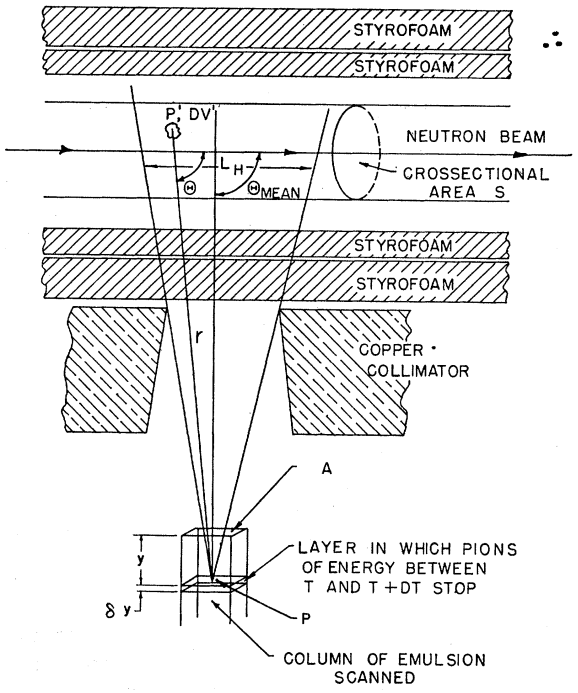

FIG. 11. Figure explaining the calculation of the laboratory cross section.

and the volume of the target by the cross section of the beam S times the active length $l_H(T)$ of the hydrogen. The active length of the hydrogen $l_H(T)$, is a function of T because the length of hydrogen seen through the collimator depends on the position of the pion ending. Then the density of endings, dn/dT, is given by:

$$\frac{dn}{dT}=N_n\rho_H A\epsilon\eta(T)f(T)\left(\frac{1}{r^2}\right)_{Av}\left(\frac{d^2\sigma_{Av}}{d\Omega dT}\right)_{Av}, \quad (10)$$

where $N_N=\nu_n\cdot S$, (the total number of neutrons incident on the target), $(1/r^2)_{Av}$ is the average of the inverse square distance over the target, and

$$\left(\frac{d^2\sigma_{Av}}{d\Omega dT}\right)_{Av}=\frac{1}{\Delta\Theta}\int_{\Theta_{min}}^{\Theta_{max}}\int_{T_N(\text{threshold})}^{T_N\max}\frac{d^2\sigma}{d\Omega dT}g(T_N)dT_N d\Theta, \quad (11)$$

where the average is carried out over the angular acceptance of the detector $\Delta\Theta$ and over the neutron energy spectrum $g(T_N)$.

IV. EXPERIMENTAL RESULTS

A. Measurement at 90°

The results of the two runs are collected in Table III. In columns 2 and 3 are given the number of pions, corrected for background, observed in the energy band listed in column 1. The active length of hydrogen determined by the geometry of the experimental arrangement is given in column 4. Columns 5, 6, and 7 give the corrections for decay in flight, and nuclear absorption in the emulsion, respectively. The calculated average of the inverse square distance is given in column 8. The experimental cross sections as determined from Eq. (11) are given in columns 9 and 10.

A total of 325 positive- and negative-pion endings were measured. No pions were observed beyond the kinematic limit for pion production from hydrogen.

The differential cross sections for $\pi^{\pm}$ production, integrated from the threshold of the detector to the kinematic limit, are:

$$\left(\frac{d\sigma}{d\Omega}\right)_{90°}^{+}=[2.296\pm0.363]\times10^{-30}\ \text{cm}^2/\text{sterad}, \quad T>14\ \text{Mev},$$

$$\left(\frac{d\sigma}{d\Omega}\right)_{90°}^{-}=[1.156\pm0.327]\times10^{-30}\ \text{cm}^2/\text{sterad}. \quad T>14\ \text{Mev}.$$

The laboratory energy spectra for $\pi^{\pm}$, calculated by using both runs, are plotted in Fig. 12(a).

A marked predominance of π^+ over π^- mesons is found at this angle. The ratio π^+/π^- is (2.01 ± 0.24). This indicates an asymmetry in the angular distribution of positive and negative pions with a preferential production of π^+ mesons at center-of-mass angles larger than 90°. This would mean, according to charge symmetry, that there should be an excess of π^- over π^+ mesons at center-of-mass angles less than 90°. Such an excess was found by Wright and Schluter[11] in their study of π^- production in $N-P$ collisions.

B. Measurement at 65°

At this angle, scanning was difficult and slow for two reasons: (1) There was a large flux of extraneous events, such as neutron stars and stray proton tracks; (2) the length of strip required to be scanned was longer than at 90° because the pion spectrum extends to higher energies. Hence only a crude measurement of the cross section was made.

The total number of pion endings found with hydrogen in the target was 22 π^+ and 50 π^- mesons. However, 2.1 π^+ and 28.6 π^- of these were due to background as determined from the run without hydrogen in the target, giving a net of 19.9 ± 1.45 π^+ and 21.4 ± 5.35 π^- from hydrogen alone. The total differential cross sections, obtained by integrating Eq. (10) from the threshold of detection to the kinematic limit, are:

$$\left(\frac{d\sigma}{d\Omega}\right)_{65°}^{+}=(1.22\pm0.30)\times10^{-30}\ \text{cm}^2/\text{sterad}, \quad T>41\ \text{Mev},$$

$$\left(\frac{d\sigma}{d\Omega}\right)_{65°}^{-}=(1.31\pm0.63)\times10^{-30}\ \text{cm}^2/\text{sterad}, \quad T>41\ \text{Mev}.$$

TABLE III. Differential cross sections for $\pi^{\pm}$ production at $\Theta=90°$.

Pion energy at center of hydrogen T_{π^c}(Mev)	No. of pions in energy band corrected for background π^+	π^-	Active length of liquid hydrogen, $l_H(T)$ (cm)	Correction for decay in flight $\eta(T)$	Correction for absorption in emulsion, $f(T)$ π^+	π^-	Effective $(1/r^2)$ (cm^{-2})	Average lab. cross section [(cm^2/sterad Mev) $\times 10^{-31}$] π^+	π^-
Run I. $N_n=(1.51\pm0.02)\times10^{11}$; $\epsilon=0.94$; $A=0.336$ cm^2; $\Theta=90°\pm15°$.									
14–20	43±6.7	18±7.0	11.6	0.946	0.999	0.999	0.002295	1.43 ±0.22	0.597±0.232
20–26	45±6.85	23±5.0	11.2	0.952	0.995	0.992	0.002217	1.60 ±0.24	0.818±0.178
26–32	22±4.69	18±4.69	10.65	0.956	0.988	0.982	0.002215	0.828±0.176	0.677±0.176
32–38	15±3.87	3±3.0	10.15	0.959	0.979	0.969	0.002030	0.651±0.168	0.13 ±0.130
38–44	6±2.44	1±1.73	9.7	0.961	0.967	0.953	0.001935	0.289±0.118	0.048±0.084
	131	63							
Run II. $N_n=(5.706\pm0.196)\times10^{11}$; $\epsilon=0.93$; $A=0.182$ cm^2; $\Theta=91°\pm5°$.									
14–20	31±5.5	12.6 ±4.6	4.71	0.946	0.999	0.999	0.001995	1.41 ±0.25	0.571±0.209
20–26	24±4.9	11.28±5.3	4.55	0.952	0.995	0.992	0.001930	1.164±0.24	0.547±0.257
26–32	19±4.35	7.64±4.0	4.35	0.956	0.988	0.982	0.001850	1.01 ±0.231	0.406±0.212
32–38	8±2.82	7.64±4.1	4.14	0.959	0.979	0.982	0.001780	0.468±0.166	0.447±0.239
38–44	4.3±2.56	5.82±3.3	3.94	0.961	0.967	0.953	0.001705	0.277±0.165	0.375±0.212
	86.3	44.98							
	217	108							

The pion spectra obtained at 65° are less reliably determined than those obtained at 90°. The histogram of the events observed at 65° is plotted in Fig. 13. The total number of π^- mesons quoted in figure have been corrected for no-prong stars.

According to the hypothesis of charge symmetry the π^+ and π^- cross sections should be equal at 90° in the center-of-mass system. The angle 65° in the laboratory corresponds to approximately 106° in the center-of-mass; therefore at 65° the number of π^+ and π^- mesons should be very nearly equal. The experimental results are consistent with this requirement of charge symmetry.

V. ANALYSIS OF DATA

The experimental cross sections can be reduced to center-of-mass cross sections for a single neutron energy provided the energy distribution of the neutron beam is known and provided the energy spectrum and angular distribution of the reaction are known. Before discussing the energy spectrum and angular distribution of the reaction, we shall make the following approximations and simplify the calculation.

(1) Because of the finite resolution $\Delta\Theta$ of the detector, to each pion energy T considered in the laboratory system there corresponds a range of energies Δt and a range of angles $\Delta\theta$ in the center-of-mass system, for a given neutron energy. The center-of-mass cross section $d^2\sigma/d\omega dt$ varies with θ and t. The angular spread $\Delta\Theta$ is small enough so that, in calculating the center-of-mass cross section for a given angle Θ in the laboratory, we may neglect the variation in $d^2\sigma(\theta,t)/d\omega dt$ with the center-of-mass angle θ and approximate the cross section $d^2\sigma(\theta,t)/d\omega dt$ by its value at the mean angle $\bar{\theta}$ calculated at the energy t in the center of mass corresponding to the angle Θ. Thus

$$\left(\frac{d^2\sigma(\theta,t)}{d\omega dt}\right)_{\Theta}\cong\frac{d^2\sigma(\bar{\theta},t(\Theta))}{d\omega dt}.$$

Then the differential cross section for production of pions in the laboratory system is given in terms of the center-of-mass cross section by

$$\left(\frac{d^2\sigma}{d\Omega dT}\right)_{T,\Theta}\cong\frac{d^2\sigma(\bar{\theta},t)}{d\omega dt}J\left(\frac{\omega,t}{\Omega,T}\right),$$

where $J(\omega,t/\Omega,T)$ is the Jacobian of the transformation from the center-of-mass system to the laboratory system.

(2) The second approximation is made by neglecting the variation with neutron energy of the center-of-mass energy t for a given pion energy T in the laboratory. This is a good approximation as long as $t>10$ Mev, as is the case for the present experiment. Hence $J(\omega,t/\Omega,T)=P/p$ (where P is the given momentum of the pion in the laboratory system and p is the corresponding momentum in the center-of-mass system) can be calculated at a mean neutron energy T_N* and used for all neutron energies.

The double integral (11) for obtaining the experimental cross section is then reduced to

$$\left(\frac{d^2\sigma_{Av}}{d\Omega dT}\right)_{Av}\cong\frac{1}{\Delta\Theta}\int\frac{P}{p}d\Theta\int\frac{d^2\sigma}{d\omega dt}(\bar{\theta},t,T_N)g(T_N)dT_N, \tag{12}$$

where in the integration over the neutron spectrum $\bar{\theta}$ and t are treated as constant. The average center-of-mass cross section is calculated from Eq. (12) approximately, replacing the average of P/p over Θ by the

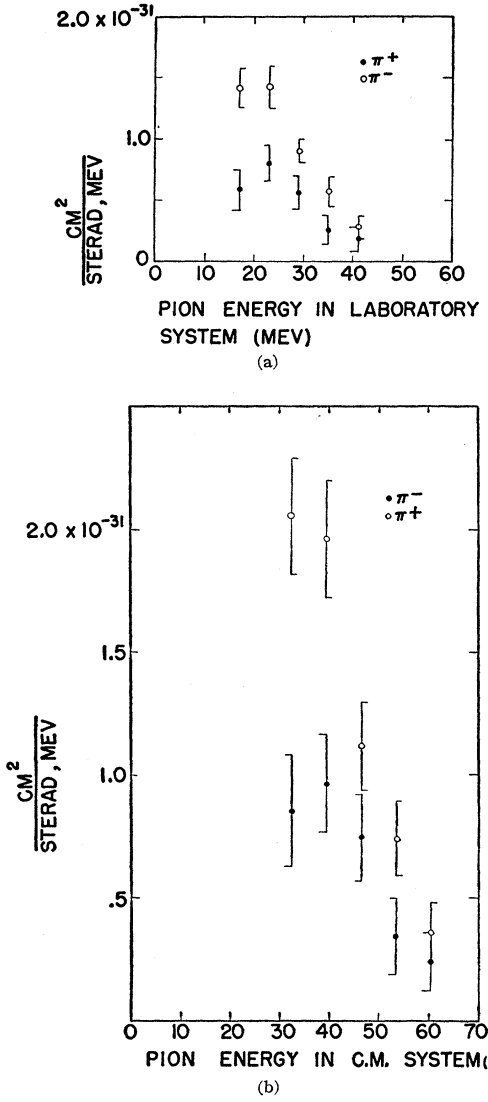

FIG. 12. (a) Average laboratory differential cross section for positive and negative pion production at 90°, due to neutrons of all energies in the beam. (b) Average center-of-mass differential cross section for positive and negative pion production at $\Theta=90°$, due to neutrons of all energies in the beam.

value of P/p at the mean angle $\bar{\theta}$.

$$\frac{d^2\sigma_{\text{Av}}}{d\omega dt}(\bar{\theta},t)\cong\left(\frac{p}{P}\right)_{\bar{\theta}}\left(\frac{d^2\sigma_{\text{Av}}}{d\Omega dT}\right)_{\text{Av}}.$$

The calculated average center-of-mass spectrum for

$$\Theta=90°(\bar{\theta}=128°)$$

is given in Fig. 12(b).

The integration over the neutron spectrum can be carried out only if the energy spectrum and the angular distribution of the cross section $d^2\sigma/d\omega dt$ is assumed. Hence we shall now discuss the nature of the energy spectrum and the angular distribution of the reaction under study.

VI. PHENOMENOLOGICAL ANALYSIS OF THE REACTION $N+P\rightarrow\pi^{\pm}$

The conservation of isotopic spin imposes severe restrictions on the production of pions in nucleon-nucleon collisions. All production processes can be described in terms of three independent reactions whose cross sections we denote by σ_{01}, σ_{11}, and σ_{10}.[30] The first subscript refers to the isotopic spin of the initial state and the second to that of the final state of the two outgoing nucleons. If the matrix elements of these three reactions are denoted by M_{01}, M_{11}, and M_{10}, then the differential cross sections for the reactions[13]

$$N+P\rightarrow\pi^-+P+P,\quad N+P\rightarrow\pi^+ +N+N$$

are given by

$$\begin{aligned}\frac{d\sigma}{d\omega}(n+p\rightarrow\pi^-)&=\frac{2\pi}{\hbar}\{\tfrac{1}{2}|M_{11}+M_{01}|^2\}\frac{dN}{dW},\\ \frac{d\sigma}{d\omega}(n+p\rightarrow\pi^+)&=\frac{2\pi}{\hbar}\{\tfrac{1}{2}|M_{11}-M_{01}|^2\}\frac{dN}{dW},\end{aligned}\tag{13}$$

where dN/dW is the density of final states and the total cross sections are given by

$$\sigma(n+p\rightarrow\pi^-)=\sigma(n+p\rightarrow\pi^+)=\tfrac{1}{2}(\sigma_{01}+\sigma_{11}).\tag{14}$$

We may consider the phenomenon of pion production to take place at a characteristic distance R from the center of the collision, where $R\sim\hbar/\mu c$. At the energies of the experiment, $p_\pi\hbar/\mu c<1$ and $p^*\hbar/\mu c<1$, where p_π is the pion momentum and p^* is the relative momentum of the nucleons in the center-of-mass system. Hence it is reasonable to limit the discussion to the production of pions and nucleons into angular momentum states with $l=0$ or 1 only.

With this limitation the allowed transitions for the reaction are determined under conservation of angular momentum and parity. The allowed transitions are given in Table IV, whose construction is the following. Consider first the σ_{01} reaction, in which the final nucleons have $T=1$; therefore if the final nucleons are in an S state, it must be a singlet state. If the pion is emitted in a p state, then the final state is $({}^1S_0,p)_{T,J}$ in which the total isotopic spin $T=0$ and the total angular momentum $J=1$. Such a state can come from two initial states of the $N-P$ system, ${}^3S_1$ and ${}^3D_1$, both of which have even parity. This is shown in row (1) of the σ_{01} reaction column.

The transition of the σ_{11} reaction written in the same row is ${}^3P_0\rightarrow({}^1S_0,s)_{1,0}$ which can interfere with the transition of the σ_{01} reaction just described. For those reactions in which only one of the matrix elements is involved, no asymmetry in the pion angular distribution can arise. In the present experiment, only the pion is

[30] A. H. Rosenfeld, Phys. Rev. **96**, 139 (1954).

observed so that, in obtaining the angular distribution of the pion, one has to integrate over the final nucleon states. Under these conditions, asymmetry in the pion angular distribution can arise due to interference between transitions of σ_{01} and σ_{11} reactions only if the spin functions of the initial states are the same and the final nucleon states are nonorthogonal. Table IV is arranged so as to list the reactions which can interfere to give asymmetry in the pion angular distribution in the same row.

In order to calculate the energy spectra and angular distributions for σ_{01} and σ_{11} reactions, it is necessary to discuss the relative importance of the transitions given in Table IV.

We first note that the meson, being a pseudoscalar particle, tends to be produced mainly in p states. Secondly, the production process is affected by two types of forces, (1) meson-nucleon force and (2) nucleon-nucleon force.

The cross section for production is proportional to the square modulus of the final nucleon wave function in a region of $\hbar/\mu c$ near the origin: $|\psi_f(r\sim\hbar/\mu c)|^2$. This is large if the nucleons are emitted in S-states where the nuclear forces enhance the wave function at the origin. Hence nucleon-nucleon forces favor the emission of nucleons in S-states rather than in P-states.

The meson-nucleon force is such that the interaction between a pion and a nucleon is greatly enhanced if they are in a state of isotopic spin $\frac{3}{2}$ and angular momentum $\frac{3}{2}$.[31] Therefore, transitions are enhanced if they

TABLE IV. Allowed transitions for the reaction $N+P\rightarrow\pi^{\pm}+2$ (nucleons).[a]

	σ_{01}			σ_{11}		
	Initial state	Parity	Final state ψ_f	Initial state	Parity	Final state ψ_f
(A)	Final nucleons in $^1S_0$ State					
1.	$^3S_1$	+	$(^1S_0,p)_{0,1}$	$^3P_0$	−	$(^1S_0,s)_{1,0}$
	$^3D_1$	+	$(^1S_0,p)_{0,1}$			
(B)	Final nucleons in $^3P_{2,1,0}$					
2.	$^1P_1$	−	$(^3P_0,p)_{0,1}$	$^1S_0$	+	$(^3P_0,s)_{1,0}$
3.				$^3P_1$	−	$(^3P_0,p)_{1,1}$
4.	$^1P_1$	−	$(^3P_1,p)_{0,1}$			
5.	$^3D_1$	+	$(^3P_1,s)_{0,1}$	$^3P_0$	−	$(^3P_1,p)_{1,0}$
				$^3P_1$	−	$(^3P_1,p)_{1,1}$
				$^3P_2$	−	$(^3P_1,p)_{1,2}$
				$^3F_2$	−	$(^3P_1,p)_{1,2}$
6.	$^1P_1$	−	$(^3P_2,p)_{0,1}$	$^1D_2$	+	$(^3P_2,s)_{1,2}$
7.	$^3D_2$	+	$(^3P_2,s)_{0,2}$	$^3P_1$	−	$(^3P_2,p)_{1,1}$
				$^3P_2$	−	$(^3P_2,p)_{1,2}$
				$^3F_2$	−	$(^3P_2,p)_{1,2}$
				$^3F_3$	−	$(^3P_2,p)_{1,3}$

[a] $\psi_{\text{final state}}=(\psi_{\text{nucleons}},\phi_{\text{meson}})_{T,J}$; ψ_{nucleons} is the state of final nucleons, S or P; ϕ_{meson} is the meson state, s or p; T is the total isotopic spin of ψ_{final}; and J is the total angular momentum of ψ_{final}.

[31] The study of pion-proton scattering shows the importance of $(\frac{3}{2},\frac{3}{2})$ state. See Anderson, Fermi, Martin, and Nagle, Phys. Rev. **91**, 155 (1953).

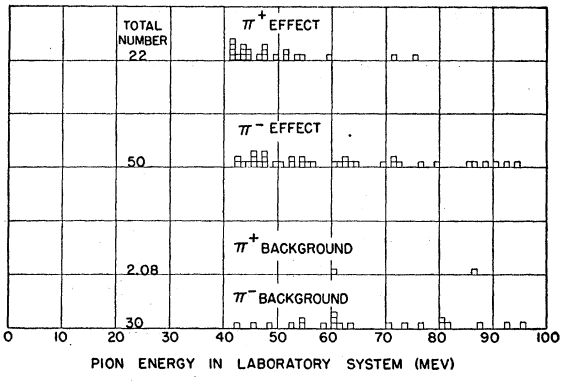

FIG. 13. Histogram of the events at 65°. In the column headed "total number," the value 30 should read 28.6.

can lead to a $(\frac{3}{2},\frac{3}{2})$ state for the pion and one of the nucleons. If the total isotopic spin of the final state has to be zero, as is the case for the σ_{01} reaction, there can be no $(\frac{3}{2},\frac{3}{2})$ enhancement. Thus enhancement due to pion-nucleon force can occur only for the σ_{11} reaction.

For the σ_{01} reaction, where no enhancement due to pion-nucleon force is possible, the most dominant transitions are assumed to be those leading to an (S,p) final state. These transitions are:

$$\left.\begin{matrix}{}^3S_1\\ {}^3D_1\end{matrix}\right\}\rightarrow(^1S_0,p)_{0,1}.$$

For the σ_{11} reaction, production into a (S,p) state is forbidden by angular momentum and parity conservation. The state (S,s) is allowed but can have no $(\frac{3}{2},\frac{3}{2})$ enhancement as the total angular momentum has to be zero. For (P,p) states enhancement due to pion-nucleon force can occur. Some information for the behavior of the σ_{11} reaction can be obtained from the study of the process $P+P\rightarrow\pi^0+P+P$. The two measurements of π^0 production at 345 Mev[7] and 430 Mev[8] seem to require a rapid energy dependence of the cross section and they are consistent with η_0^6 to η_0^8 variation of the cross section, where η_0 is the maximum pion momentum in the center-of-mass system, for a given neutron energy. Such an energy dependence can only arise from both the meson and nucleon both being emitted in P-states (see discussion below). Therefore it is assumed that transitions leading to (P,p) states are dominant for the σ_{11} reaction.

A. Angular Distributions

Since we consider only mesons produced in s- and p-states, the differential cross sections for the pure reactions σ_{01} and σ_{11} are, in general,

$$(d^2\sigma/d\omega dt)_{01}=A_{01}(t,t_0)+C_{01}(t,t_0)\cos^2\theta, \quad (15a)$$

$$(d^2\sigma/d\omega dt)_{11}=A_{11}(t,t_0)+C_{11}(t,t_0)\cos^2\theta, \quad (15b)$$

where t_0 is the maximum pion energy in the center-of-mass system for a given neutron energy T_N. In obtaining the angular distribution for either π^+ or π^- production, asymmetry can arise due to interference between transitions of the σ_{01} and σ_{11} reactions.

The dominant states $(^1S_0,\phi)_{0,1}$ and $(^3P_1,\phi)_{1,J}$ cannot interfere; hence asymmetry has to arise from other nondominant states, such as $(^1S_0,s)_{1,0}$ or $(^3P_1,s)_{0,1}$, interfering with the dominant states. The amount of admixture needed to give sizable asymmetry can be very small; consequently the contribution of the nondominant states to the total cross section would be negligible. Thus the constant term A and the coefficient C of the $\cos^2\theta$ term will be little affected by the presence of these interfering states. The constant term A and the coefficient C of the $\cos^2\theta$ term in the differential cross section for the π^+ or π^- angular distribution will therefor be proportional to each other; e.g.,

$$C_{01}=k_{01}A_{01}.$$

Hence we may write for the differential cross section for the production of negative pions:

$$2(d^2\sigma/d\omega dt)^-=\{1+k_{01}\cos^2\theta\}A_{01}(t,t_0)+(1+k_{11}\cos^2\theta)A_{11}(t,t_0)+B(t,t_0)\cos\theta. \quad (16a)$$

The asymmetry is given by the $\cos\theta$ term.

The coefficient of the $\cos\theta$ term has a different energy spectrum from both A_{01} and A_{11}. By charge symmetry, the corresponding equation for π^+ production is

$$2(d^2\sigma/d\omega dt)^+=(1+k_{01}\cos^2\theta)A_{01}(t,t_0)+(1+k_{11}\cos^2\theta)A_{11}(t,t_0)-B(t,t_0)\cos\theta. \quad (16b)$$

B. Energy Spectra

Let us define the pion energy spectra due to the dominant transitions of the reactions σ_{01} and σ_{11} as f_u and f_v respectively; then

$$A_{01}=h_{01}f_u(t,t_0); \quad A_{11}=h_{11}f_v(t,t_0), \quad (17a)$$

where h_{01} and h_{11} are constants.

Let us define the energy spectrum $B(t,t_0)$ by f_w; then

$$B(t,t_0)=k_wf_w(t,t_0), \quad (17b)$$

where k_w is a constant.

The final states assumed for the dominant transitions are $(^1S_0,\phi)_{0,1}$ for σ_{01} and $(^3P_1,\phi)_{1,J}$ for σ_{11} reactions, respectively. In calculating the energy spectra, the effects of final-state interactions have to be taken into account. There are two types of interactions which have to be considered: the meson-nucleon and the nucleon-nucleon interactions, respectively.

The meson-nucleon force is taken into account qualitatively in determining what states are dominant, and quantitatively in calculating the energy dependence of the cross section using the known variation of phase shift with energy. The distortion of the wave function from a plane wave due to the meson-nucleon force is not calculated in detail, but it is assumed that at the energies of the experiment this correction is energy-independent.

The nucleon-nucleon force is well known for the $^1S_0$ state, and it is taken into account in calculating the energy spectra following the method of phonomenological analysis given by Watson and others.[30,32] The pion spectrum, for a given neutron energy, for transitions leading to an $(^1S_0,\phi)_{0,1}$ state is given by[30]:

$$f_u(t,t_0)=\Lambda_u\frac{\eta^3(t_0-t)^{\frac{1}{2}}}{|B|+t_0-t}; \quad \Lambda_u=\frac{8}{3\pi}\left(\frac{2}{\mu}\right)^{\frac{1}{2}}; \quad (18)$$

where μ is the pion mass, $|B|$ is the binding energy of the nucleons in $^1S_0$ state and t_0 the maximum pion energy; η is the pion momentum in μc units; and t is the pion energy in the center-of-mass system. The constant Λ_u is so determined that in the nonrelativistic limit the integral of $f_u(t,t_0)$ from zero to the maximum energy t_0 is given by

$$\int_0^{t_0}f_u(t,t_0)dt\simeq\eta_0^4(1+\cdots),$$

where η_0 is the maximum pion momentum in μc units in the center-of-mass system. The numerator of (18) is the product of η^2/γ from the square of the matrix element for the production of a p-state pion and $\eta(t_0-t)^{\frac{1}{2}}\gamma$ which is the phase space available to the three final particles, where γ is the total pion energy in μc^2 units. The nucleon-nucleon force introduces the denominator[32] $(|B|+t_0-t)$.

For transitions leading to (P,ϕ) states the effect of nuclear force is neglected, and therefore the denominator is absent. As the nucleons are emitted in P states the relative momentum of the nucleons appears in the matrix element. The resulting pion spectrum is

$$f_v(t,t_0)=\Lambda_v\eta^3(t_0-t)^{3/2}; \quad \Lambda_v=\frac{64}{3\pi}\left(\frac{4}{\mu}\right)^{5/2}, \quad (19)$$

where Λ_v is determined in the same way as for the previous spectrum, i.e., by requiring that

$$\int_0^{t_0}f_v(t,t_0)dt\cong\eta_0^3(1+\cdots)$$

in the nonrelativistic limit.

The asymmetry can arise from interactions between two nondominant states, e.g., $(^3P_0,\phi)_{0,1}$ with $(^3P_0,s)_{1,0}$, or between a dominant state and a nondominant state, e.g., $(^1S_0,\phi)_{0,1}$ with $(^1S_0,s)_{1,0}$. We shall neglect the contribution from the interaction between the two nondominant states. Then $B(t,t_0)$ is made up of two types

[32] K. M. Watson, Phys. Rev. **88**, 1163 (1952); and Aitken, Mahmoud, Henley, Ruderman, and Watson, Phys. Rev. **93**, 1349 (1954).

of terms: (1) a term due to interference of an (S,p) state of σ_{01} with an (S,s) state of σ_{11} reaction, and (2) a term due to interference of a (P,p) state of reaction σ_{11} with a (P,p) state of σ_{01} reaction. Following phenomenological analysis similar to that used for the pure isotopic spin reactions, we obtain the energy spectra for the coefficient of the $\cos\theta$ term. The energy spectrum for the term of type (1) is

$$f_{w1}=\Lambda_{w1}\frac{\eta^2(t_0-t)^{\frac{1}{2}}}{|B|+t_0+t};\quad \Lambda_{w1}=\frac{3}{\sqrt{8}}\frac{1}{\sqrt{\mu}} \tag{20}$$

and that for the term of type (2) is

$$f_{w2}=\Lambda_{w2}\eta^2(t_0-t)^{3/2};\quad \Lambda_{w2}=\frac{35}{\sqrt{2}}\frac{1}{\mu^{5/2}}. \tag{21}$$

Therefore coefficient $B(t,t_0)$ is given by

$$B(t,t_0)=kf_w(t,t_0)=k_{w1}f_{w1}+k_{w2}f_{w2},$$

where k_{w1} and k_{w2} are constants.

The total cross section is best analyzed in terms of the sum of positive- and negative-pion cross sections, where the interference term does not appear. From Eqs. (16a) and (16b), we get

$$(d^2\sigma/d\omega dt)^+ + (d^2\sigma/d\omega dt)^- = (a_1+b_1\cos^2\theta)f_u(t,t_0) + (a_2+b_2\cos^2\theta)f_v(t,t_0), \tag{22}$$

where $a_1=h_{01}$, $b_1=h_{01}k_{01}$, $a_2=h_{11}$, $b_2=h_{11}k_{11}$. Integrating over the pion energy spectrum, we get the differential cross section for $(\pi^+ + \pi^-)$ to be:

$$(d\sigma/d\omega)^+ + (d\sigma/d\omega)^- = (a_1+b_1\cos^2\theta)\left[4Z^2\left(1-\frac{Z}{4(2+Z)}\right)\left(1+\frac{Z}{2}\right)^2\right] + (a_2+b_2\cos^2\theta)[16Z^4(1+3Z/8)], \tag{23}$$

where $Z=t_0/\mu c^2$.

The asymmetry is directly measured by the difference of the positive- and negative-pion cross sections. From Eqs. (16a) and (16b), we get

$$(d^2\sigma/d\omega dt)^+ - (d^2\sigma/d\omega dt)^- = -B(t,t_0)\cos\theta = -[k_{w1}f_{w1}+k_{w2}f_{w2}]\cos\theta. \tag{24}$$

By integrating over the pion energy, the magnitude of the interference term at any angle is obtained to be

$$(d\sigma/d\omega)^+ - (d\sigma/d\omega)^- = -\{k_{w1}[2\sqrt{2}Z^{3/2}(1+\tfrac{2}{5}Z_0 - \tfrac{3}{8}\pi(2+Z_0)\sqrt{b})]+k_{w2}[8\sqrt{2}Z^{7/2}(1+2Z/9)]\}\cos\theta, \tag{25}$$

where $Z=t_0/\mu c^2$; $b=|B|/t_0$.

At nonrelativistic energies these differential cross sections become

$$(d\sigma/d\omega)^+ + (d\sigma/d\omega)^- \cong (a_1+b_1\cos^2\theta)\eta_0^4 + (a_2+b_2\cos^2\theta)\eta_0^8, \tag{23a}$$

$$(d\sigma/d\omega)^+ - (d\sigma/d\omega)^- \cong -(k_{w1}\eta_0^3+k_{w2}\eta_0^7)\cos\theta, \tag{25a}$$

where η_0 is the maximum momentum of the pion in the center-of-mass system in μc units for a given neutron energy.

VII. CALCULATION OF CENTER-OF-MASS CROSS SECTIONS AT A SINGLE NEUTRON ENERGY

A. Total Cross Section

The experimental cross sections for the sum of positive and negative pions at any angle are now expressed in terms of the center-of-mass cross section. The integration over the neutron spectrum and the average over the angular acceptance in Eq. (12) is then carried out. By using Eq. (22), Eq. (12) becomes:

$$[(d^2\sigma/d\Omega dT)^+ + (d^2\sigma/d\Omega dT)^-]_{Av} = \frac{1}{\Delta\Theta}\int_{\Theta_{\min}}^{\Theta_{\max}}\frac{P}{p}d\Theta\int_0^{t_{0\max}}\{(a_1+b_1\cos^2\bar{\theta})f_u + (a_2+b_2\cos^2\bar{\theta})f_v\}g(t_0)dt_0.$$

The effective pion spectra $u(t)$ and $v(t)$ in the center-of-mass system are defined by

$$u(t)=\int_0^{t_{0\max}} f_u(t,t_0)g(t_0)dt_0,$$

$$v(t)=\int_0^{t_{0\max}} f_v(t,t_0)g(t_0)dt_0.$$

The experimental cross section is then given by

$$[(d^2\sigma_{Av}/d\Omega dT)^+ + (d^2\sigma_{Av}/d\Omega dT)^-]_\Theta = a_1\alpha_1(T,\Theta) + b_1\beta_1(T,\Theta) + a_2\alpha_2(T,\Theta) + b_2\beta_2(T,\Theta), \tag{26}$$

where α_1, β_1, α_2, and β_2 are the effective pion spectra transformed to the laboratory system and averaged over the angular acceptance, after being multiplied by the appropriate weighting factor of unity or $\cos^2\theta$. They are given by

$$\alpha_1(T,\Theta)=\frac{1}{\Delta\Theta}\int_{\Theta_{\min}}^{\Theta_{\max}}d\Theta\frac{P}{p}u(t),$$

$$\alpha_2(T,\Theta)=\frac{1}{\Delta\Theta}\int_{\Theta_{\min}}^{\Theta_{\max}}d\Theta\frac{P}{p}v(t),$$

$$\beta_1(T,\Theta)=\frac{1}{\Delta\Theta}\int_{\Theta_{\min}}^{\Theta_{\max}}d\Theta\frac{P}{p}\cos^2\bar{\theta}u(t),$$

$$\beta_2(T,\Theta)=\frac{1}{\Delta\Theta}\int_{\Theta_{\min}}^{\Theta_{\max}}d\Theta\frac{P}{p}\cos^2\bar{\theta}v(t).$$

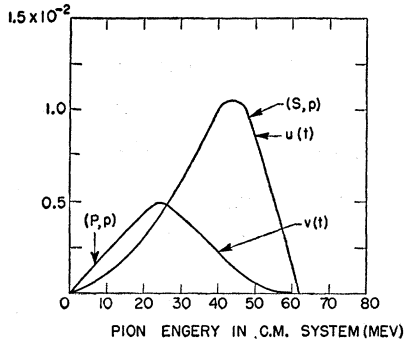

FIG. 14. Effective pion spectra $u(t)$ and $v(t)$ in the center-of-mass system.

The effective pion spectra in the center-of-mass system, $u(t)$ and $v(t)$ for the (S,p) and the (P,p) states respectively are shown in Fig. 14. The laboratory functions α_1, β_1, α_2, and β_2 calculated at the two angles of the experiment, 90° and 65°, are shown in Figs. 15 and 16. They are calculated for pion energies greater than the threshold of the detector.

The coefficients a_1, b_1, a_2, b_2 can be determined from the experimental spectrum for $(\pi^+ + \pi^-)$ at 90° alone. However, the functions α_1, β_1 and α_2, β_2 are sufficiently similar in shape to make it impossible to evaluate a_1 b_1 or a_2 and b_2 separately from the 90° data alone. Moreover it is a good approximation to take functions α_1, β_1 and α_2, β_2 to be proportional to each other, i.e.,

$$\beta_1 = l_1\alpha_1, \quad \beta_2 = l_2\alpha \quad \text{for } \Theta = 90°,$$

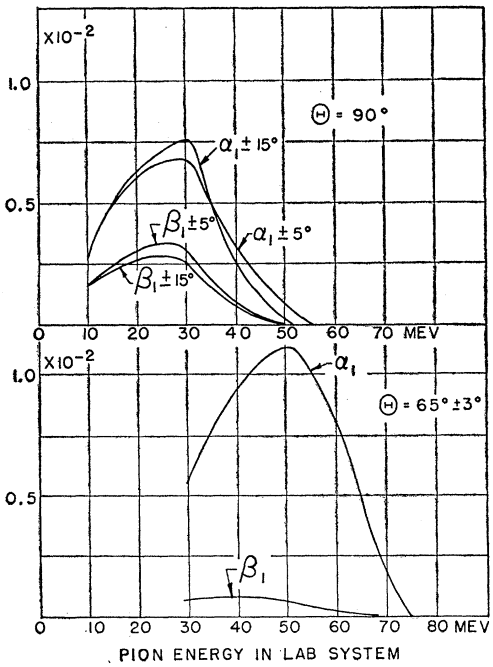

FIG. 15. Effective pion spectra for the two runs transformed to the laboratory system and averaged over the angular acceptance, for the (S,p) final states.

where l_1 and l_2 are constants, whose value is equal to the average of $\cos^2\theta$; then the 90° cross section can be written as:

$$[(d^2\sigma_{Av}/d\Omega dT)^+ + (d^2\sigma_{Av}/d\Omega dT)^-]_{90°} = C_1\alpha_1(T,90°) + C_2\alpha_2(T,90°), \quad (27)$$

where $C_1 = a_1 + l_1b_1$, $C_2 = a_2 + l_2b_2$; $l_1 = l_2 = \langle\cos^2\theta\rangle_{Av} = 0.36$.

The mean 90° spectrum for the sum of positive and negative pions was fitted, using a least-squares method, by the function previously given. In the analysis the results of the two runs were combined and the density of events

$$(dn/dT)^+ + (dn/dT)^-$$

was expressed in terms of the functions α_1 and α_2 calculated for the different geometries of the two runs. Thus the combined density of events is given by

$$\left(\frac{dn}{dT}\right)^+ + \left(\frac{dn}{dT}\right)^- = C_1\left\{\frac{\alpha_{11}}{G_1} + \frac{\alpha_{12}}{G_2}\right\} + C_2\left\{\frac{\alpha_{21}}{G_1} + \frac{\alpha_{22}}{G_2}\right\},$$

where the factor G is obtained from Eq. (10) as

$$G = N_n\rho_H\epsilon\eta f l_H(1/r^2)_{Av},$$

and G_1, α_{11}, α_{12}, and G_2, α_{21}, α_{22} are the values of G, α_1, and α_2 calculated for the two runs respectively. Table V gives the pertinent data for the least-squares analysis. In estimating the error in dn/dT, the errors in determining the length of hydrogen and in the number of neutrons incident are taken into account.

The values of the coefficients determined are:

$$C_1 = (1.57 \pm 0.35) \times 10^{-29} \text{ cm}^2/\text{sterad},$$
$$C_2 = (4.87 \pm 2.05) \times 10^{-29} \text{ cm}^2/\text{sterad}.$$

The correlation coefficient $\langle\Delta C_1 \Delta C_2\rangle_{Av}$ is equal to 0.305×10^{-58}. The weighted least-square sum

$$M = \sum(\Delta_i/X_i)^2,$$

where Δ_i are the deviation of the calculated value from the experimental value and X_i are the experimental errors in the ith measurement, was found to be 1.15. As the degrees of freedom for fitting are 3 this indicates a good fit to the data.

The smallness of the contribution of the $\cos^2\theta$ term at 65° is evident from the comparison of areas under the β_1, β_2 curves and α_1, α_2 curves in Figs. 15(b) and 16(b). Hence neglecting the β_1 and β_2 terms we may write the 65° cross section as:

$$[(d^2\sigma_{Av}/d\Omega dT)^+ + (d^2\sigma_{Av}/d\Omega dT)^-]_{65°} = a_1\alpha_1(T,65°) + a_2\alpha_2(T,65°).$$

A most probable fit of this function to the events observed was made using the method of maximum likelihood and the best values for coefficients a_1 and a_2 were

TABLE V. Density of $(\pi^+ + \pi^-)$ events at 90° in the laboratory system, and values of functions $\{(\alpha_{11}/G_1)+(\alpha_{12}/G_2)\}$ and $\{(\alpha_{21}/G_1)+(\alpha_{22}/G_2)\}$ used to calculate the coefficients C_1 and C_2.

Pion energy at center of hydrogen (Mev)	Total number of $(\pi^+ + \pi^-)$ mesons in energy band for both runs corrected for background	G_1 (In units of 10^{-32} cm² per sterad)	G_2	α_{11}/G_1	α_{12}/G_2 (In units of 10^{29} per Mev)	α_{21}/G_1	α_{22}/G_2
14–20	104.6 ±12.0	1.99	2.72	2.65	2.0	1.215	0.890
20–26	102.3 ±12.3	2.14	2.91	2.95	2.23	0.874	0.584
26–32	65.6 ± 9.5	2.26	3.19	2.92	2.26	0.451	0.256
32–38	33.64± 6.6	2.61	3.51	1.85	1.21	0.160	0.0855
38–44	16.12± 5.05	2.90	3.87	0.912	0.512	0.0231	0

found to be

$$a_1=(0.134\pm0.36)\times10^{-29}\ \text{cm}^2/\text{sterad},$$
$$a_2=(7.08\pm2.58)\times10^{-29}\ \text{cm}^2/\text{sterad}.$$

The correlation coefficient $\langle\Delta a_1\Delta a_2\rangle_{\text{Av}}$ is equal to -0.58×10^{-58}. Combining these with the values of C_1 and C_2 determined above, we obtain the values for the coefficients of the $\cos^2\theta$ term to be

$$b_1=(3.99\pm1.37)\times10^{-29}\ \text{cm}^2/\text{sterad},$$
$$b_2=(-6.14\pm9.1)\times10^{-29}\ \text{cm}^2/\text{sterad}.$$

The correlation coefficient $\langle\Delta b_1\Delta b_2\rangle_{\text{Av}}$ is equal to -8.04×10^{-58}.

The center-of-mass differential cross section for the production of $(\pi^+ + \pi^-)$ mesons at a single neutron energy $T_N(t_0)$ is given by

$$(d^2\sigma/d\omega dT)^+ + (d^2\sigma/d\omega dT)^- = \{(0.134\pm0.36)+(3.99\pm1.37)\cos^2\theta\}f_u + \{(7.08\pm2.58)+(-6.41\pm9.1)\cos^2\theta\}f_v \times10^{-29}\ \text{cm}^2/\text{sterad Mev}.$$

The total cross section for the production of $(\pi^+ + \pi^-)$ mesons is obtained by integrating over the energy and the angle of the pion:

$$\sigma(\pi^+ + \pi^-)=4\pi\left\{(1.46\pm0.56)\int_0^{t_0} f_u dt + (5.04\pm3.96)\int_0^{t_0} f_v dt\right\}\times10^{-29}\ \text{cm}^2.$$

This is evaluated at a neutron energy for which the result is least sensitive to the exact shape of the energy spectra and excitation functions. At $T_N=409$ Mev, the pure-isotopic-spin-reaction cross sections are calculated to be:

$$\sigma_{01}=(0.134\pm0.051)\ \text{mb},\quad \sigma_{11}=(0.183\pm0.143)\ \text{mb}.$$

Hence the total cross section is

$$\sigma(\pi^+ + \pi^-)=\sigma_{01}+\sigma_{11}=(0.317\pm0.147)\ \text{mb}. \quad (28)$$

From the experimental cross section at $\Theta=90°$ coefficients C_1 and C_2 have been calculated, and the differential cross section at the corresponding center-of-mass angle is

$$\left[\left(\frac{d\sigma}{d\omega}\right)^+ + \left(\frac{d\sigma}{d\omega}\right)^-\right]_{\Theta=90°} = (a_1+b_1\langle\cos^2\theta\rangle_{\text{Av}})\int_0^{t_0} f_u dt + (a_2+b_2\langle\cos^2\theta\rangle_{\text{Av}})\int_0^{t_0} f_v dt,$$

where θ is such that $\langle\cos^2\theta\rangle_{\text{Av}}=0.36$ or almost equal to $\frac{1}{3}$. Hence the total cross section can be obtained directly from their differential cross section by

$$\sigma(\pi^+ + \pi^-)=4\pi[(d\sigma/d\omega)^+ + (d\sigma/d\omega)^-]_{90°};$$

at $T_N=409$ Mev this is

$$\sigma(\pi^+ + \pi^-)=(0.321\pm0.082)\ \text{mb}. \quad (29)$$

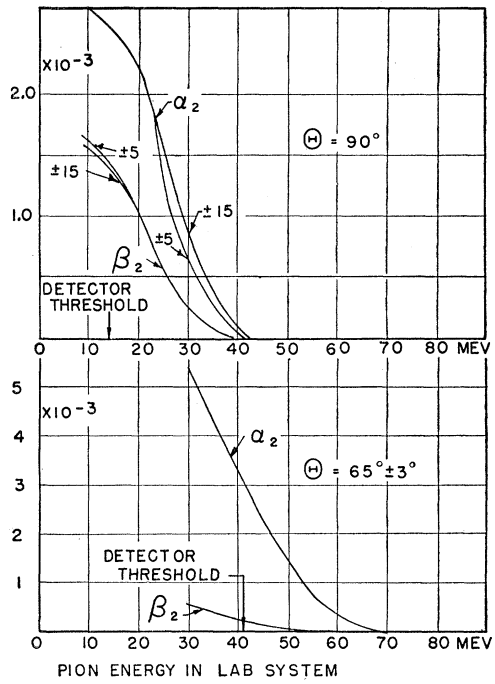

FIG. 16. Effective pion spectra for the two runs transformed to the laboratory system and averaged over the angular acceptance for the $(P,\dot{p})$ final states.

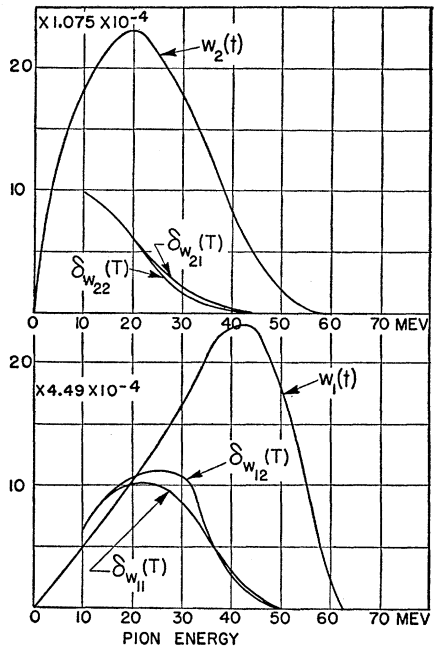

FIG. 17. Effective pion spectra in the center-of-mass system and transformed to the laboratory system for two types of interference terms.

This more accurate value is in agreement with that fetermined using the complete angular distribution obtained from both the 90° and 65° data [Eq. (28)].

Using Eq. (14) the total cross section for π^+ or π^- production is

$$\sigma(\pi^+)=\sigma(\pi^-)=\tfrac{1}{2}\sigma(\pi^++\pi^-)=(0.16\pm0.04)\text{ millibarn}$$

at $T_N=409$ Mev.

B. Asymmetry

By using Eq. (24) for the difference of the positive- and negative-pion cross sections in the center-of-mass system, the corresponding difference in the laboratory system is obtained from Eq. (12) as:

$$[(d^2\sigma_{Av}/d\Omega dT)^+-(d^2\sigma_{Av}/d\Omega dT)^-]_\Theta$$
$$=\frac{1}{\Delta\Theta}\int_{\Theta\min}^{\Theta\max}\frac{P}{p}\cos\bar{\theta}d[k_{w1}W_1(t)+k_{w2}W_2(t)]$$
$$=k_{w1}\delta w_1(T,\Theta)+k_{w2}\delta w_2(T,\Theta), \qquad (30)$$

where $W_1(t)$ and $W_2(t)$ are the effective pion spectra in the center-of-mass system, given by

$$W_1(t)=\int_0^{t_0\max} f_{w1}(t,t_0)g(t_0)dt_0;$$

$$W_2(t)=\int_0^{t_0\max} f_{w2}(t,t_0)g(t_0)dt_0,$$

and the corresponding laboratory functions are given by

$$\delta w_1(T,\Theta)=\frac{1}{\Delta\Theta}\int_{\Theta\min}^{\Theta\max}\frac{P}{p}\cos\bar{\theta}w_1(t)d\Theta,$$

$$\delta w_2(T,\Theta)=\frac{1}{\Delta\Theta}\int_{\Theta\min}^{\Theta\max}\frac{P}{p}\cos\bar{\theta}w_2(t)d\Theta.$$

All these four functions w_1, w_2, δw_1, and δw_2 are shown in Fig. 17 calculated for $\Theta=90°$ for the two runs.

The mean 90° spectrum for the difference of π^+ and π^- mesons was fitted, by using a least-squares method, with the function given in Eq. (30). Here again in analyzing the data, the results of the two runs were combined and the total density of $(\pi^+-\pi^-)$ events was expressed in terms of the functions δw_1 and δw_2 by the equation

$$\frac{dn^+}{dT}-\frac{dn^-}{dT}=k_{w1}\left\{\frac{\delta w_{11}}{G_1}+\frac{\delta w_{12}}{G_2}\right\}+k_{w2}\left\{\frac{\delta w_{21}}{G_1}+\frac{\delta w_{22}}{G_2}\right\},$$

where G is the same factor as defined in the analysis of the sum of $(\pi^++\pi^-)$ events, G_1, δw_{11}, δw_{12} and G_2, δw_{21}, δw_{22} are the values of G, δw_1, and δw_2 calculated for the geometries of the two runs respectively. The data required for the least-squares analysis of the difference spectrum are given in Table VI. The values of the coefficients k_{w1} and k_{w2} are determined to be:

$$k_{w1}=(0.72\pm0.54)\times10^{-29}\text{ cm}^2/\text{sterad},$$
$$k_{w2}=(6.98\pm4.77)\times10^{-29}\text{ cm}^2/\text{sterad}.$$

The correlation coefficient $\langle\Delta k_{w1}\Delta k_{w2}\rangle_{Av}$ is equal to $-2.28\ 10^{-58}$. The weighted least-squares sum $M=\sum(\Delta_i/X_i)^2$ is 0.02 and the degrees of freedom one.

The coefficient of the $\cos\theta$ term is given by

$$B(t,t_0)=\{(0.72\pm0.54)f_{w1}+(6.98\pm4.77)f_{w2}\}\times10^{-29}\text{ cm}^2/\text{sterad Mev}.$$

The coefficient integrated over the pion energy, for the neutron energy $T_N=409$ Mev, is

$$\int_0^{t_0}B(t,t_0)dt=(2.763\pm1.59)\times10^{-29}\text{ cm}^2/\text{sterad}.$$

Therefore the differential cross section for charged pion production in neutron-proton collisions at a single neutron energy $T_N(t_0)$ is determined to be:

$$(d^2\sigma/d\omega dt)^\pm$$
$$=\{[(0.067\pm0.18)f_u+(3.54\pm1.29)f_v]$$
$$+[(2.0\pm0.69)f_u+(-3.07\pm4.5)f_v]\cos^2\theta$$
$$\mp[(0.36\pm0.27)f_{w1}+(3.49\pm2.39)f_{w2}]\cos\theta\}\times10^{-29}\text{ cm}^2/\text{sterad Mev}.$$

The differential cross section, integrated over pion energy, for a single neutron energy $T_N=409$ Mev, is

calculated to be

$$(d\sigma/d\omega)^{\pm}=\{(1.07\pm0.39)\mp(1.38\pm0.78)\cos\theta + (0.57\pm1.40)\cos^2\theta\}\times10^{-29}\ \text{cm}^2/\text{sterad}.$$

VIII. CONCLUSIONS

The differential cross sections and energy spectra for the production of charged pions in neutron-proton collisions have been measured at two laboratory angles, $\Theta=90°$ and 65°. The number of positive and negative pions at 65° (corresponds to 90° in the center-of-mass system) are roughly equal, while at 90° the ratio of positive to negative pions is 2.01 ± 0.24.

The total cross section for π^+ or π^- production at the neutron energy $T_N=409$ Mev is determined to be

$$\sigma(\pi^+)=\sigma(\pi^-)=(0.16\pm0.04)\ \text{mb}.$$

Because of the experimental low-energy cutoff for the pions, $\frac{2}{3}$ at most of the total pion energy spectrum at each angle was observed. Further, the pions observed were produced by neutrons of all energies from threshold for pion production to the maximum energy in the neutron beam. Hence, in orer to calculate the cross section at a single neutron energy, it was necessary to assume reasonable energy spectra and excitation functions for the reaction. This was done in a phenomenological way under the hypothesis of charge independence. From the experimental results, the contributions from these various assumed spectra were determined and the above total cross section calculated at a single neutron energy. The cross section is quoted at a neutron energy for which the result is least sensitive to the exact shape for the energy spectra and the excitation functions assumed. This is possible because the neutron beam has a sharp high-energy peak in its spectrum.

The angular distribution in the center-of-mass system at neutron energy $T_N(t_0)=409$ Mev was determined to be:

$$(d\sigma/d\omega)^{\pm}=\{(1.07\pm0.39)\mp(1.38\pm0.78)\cos\theta + (0.57\pm1.4)\cos^2\theta\}\times10^{-29}\ \text{cm}^2/\text{sterad}.$$

TABLE VI. Density of $(\pi^+-\pi^-)$ events at 90° in the laboratory system, and values of functions $(\delta\omega_{11}/G_1)+(\delta\omega_{12}/G_2)$ and $(\delta\omega_{21}/G_1)+(\delta\omega_{22}/G_2)$ used to calculate the coefficients $k\omega_1$ and $k\omega_2$.

Pion energy at center of hydrogen (Mev)	Total number of $(\pi^+-\pi^-)$ mesons in energy band for both runs corrected for background	G_1 (In units of 10^{-32} cm² per sterad)	G_2	$\left[\frac{\delta\omega_{11}}{G_1}+\frac{\delta\omega_{12}}{G_2}\right]$ (In units of 10^{29} per Mev)	$\left[\frac{\delta\omega_{21}}{G_1}+\frac{\delta\omega_{22}}{G_2}\right]$ (In units of 10^{29} per Mev)
14.0–21.5	55.2 ±12.5	2.015	2.750	3.807	0.6582
21.5–31.5	44.1 ±13.1	2.26	3.085	3.471	0.2621
31.5–50.0	15.05± 8.25	2.92	3.89	0.7748	0.0300

In determining the coefficient of the $\cos\theta$ term there is a large uncertainty not shown by the error quoted, which is due to the lack of knowledge of the number of states contributing.

The cross sections for the pure isotopic spin reactions σ_{01} and σ_{11} are calculated to be:

$$\sigma_{01}=(0.131\pm0.051)\ \text{mb},\quad \sigma_{11}=(0.183\pm0.143)\ \text{mb},$$

$$\text{at } T_N=409\ \text{Mev}.$$

It is seen that at the energy of the experiment the magnitude of the σ_{11} cross section is comparable to the σ_{01} cross section. The value for the σ_{11} cross section can be compared to the value estimated by Rosenfeld[30] from the measurement of the cross section of π^0 production in proton-proton collisions at 345 and 430 Mev. The estimated value of 0.1 mb is consistent with (0.183 ± 0.143) mb determined in this experiment.

IX. ACKNOWLEDGMENTS

It is indeed a great pleasure to acknowledge the excellent guidance of Professor H. L. Anderson throughout this research. I wish to thank Dr. Roger H. Hildebrand for his interest in the problem and for his active help throughout the course of the experiment. I also thank Dr. Arthur Rosenfeld and Dr. Frank Solmitz for many stimulating discussions and useful suggestions. Thanks are due to Tadao Fujii and Joseph Fainberg, for their help in conducting the experiment and assembling the equipment; to the cyclotron staff for their excellent cooperation during the experiment; and to the scanners J. T. Lach and Meera Backus.